

# Efficient unidirectional nanoslit couplers for surface plasmons

F. López-Tejiera,<sup>1</sup> Sergio G. Rodrigo,<sup>1</sup> L. Martín-Moreno,<sup>1,\*</sup> F. J. García-Vidal,<sup>2</sup> E. Devaux,<sup>3</sup> T. W. Ebbesen,<sup>3</sup> J. R. Krenn,<sup>4</sup> I. P. Radko,<sup>5</sup> S. I. Bozhevolnyi,<sup>5</sup> M. U. Gonzalez,<sup>6</sup> J. C. Weeber,<sup>6</sup> and A. Dereux<sup>6</sup>

<sup>1</sup>*Departamento de Física de la Materia Condensada-ICMA,  
Universidad de Zaragoza, E-50009 Zaragoza, Spain*

<sup>2</sup>*Departamento de Física Teórica de la Materia Condensada,  
Universidad Autónoma de Madrid, E-28049 Madrid, Spain*

<sup>3</sup>*Laboratoire de Nanostructures, ISIS,  
Université Louis Pasteur, F-67000 Strasbourg, France*

<sup>4</sup>*Institute of Physics, Karl Franzens University,  
Universitätsplatz 5, A-8010 Graz, Austria*

<sup>5</sup>*Department of Physics and Nanotechnology,  
Aalborg University, DK-9220 Aalborg, Denmark*

<sup>6</sup>*Laboratoire de Physique de l' Université de Bourgogne,  
UMR CNRS 5027, F-21078 Dijon, France*

---

\*Electronic address: lmm@unizar.es

Plasmonics is based on surface plasmon polariton (SPP) modes which can be laterally confined below the diffraction limit, thereby enabling ultracompact optical components[1, 2]. In order to exploit this potential, the fundamental bottleneck of poor light-SPP coupling must be overcome. In established SPP sources (using prism[3, 4], grating[5] or nanodefekt[6] coupling) incident light is a source of noise for the SPP, unless the illumination occurs away from the region of interest, increasing the system size and weakening the SPP intensity. Back-side illumination of subwavelength apertures in optically thick metal films[7, 8, 9, 10, 11, 12, 13] eliminates this problem but does not ensure a unique propagation direction for the SPP. We propose a novel back-side slit-illumination method based on drilling a periodic array of indentations at one side of the slit. We demonstrate that the SPP running in the array direction can be suppressed, and the one propagating in the opposite direction enhanced, providing localized unidirectional SPP launching.

A picture of the proposed SPP-launcher is shown in Figure 1. A periodic array of one-dimensional (1D) indentations is fabricated at the (output) metal surface close and parallel to the illuminated slit. The design of this device is based on two facts. The first one is that the reflection of SPPs by a periodic array of indentations presents maxima at the low- $\lambda$  edges of the plasmonic bandgaps [14, 15]. For subwavelength indentations, the spectral locations of these edges can be obtained by folding the dispersion relation of SPPs for a *flat* metal surface into the first Brillouin zone, satisfying the following expression:

$$k_p P = m\pi, \tag{1}$$

where  $P$  is the period of the array,  $k_p$  holds for in-plane plasmon wave-vector and  $m$  is the band index. Remarkably, although the reflectance maxima depends on groove geometry (width and depth) and number of grooves, their spectral locations do not.

The second fact is that the phase picked up by the SPP upon reflection is just  $m\pi$ , precisely at the condition given by Eq.(1), as obtained by the modal expansion developed in Ref. [15]. Using these two results, a very simple scheme for the efficient unidirectional launching of SPPs can be envisaged. For a given frequency, by choosing  $P$  such that condition given by equation (1) is fulfilled, a SPP emerging from the slit to the left side will be mainly back-scattered. The interference of this reflected SPP with the one leaving the

slit to the right can be tuned by adjusting the separation,  $d$ , between the slit and the first groove of the array (defined centre to centre). The total phase difference,  $\phi$ , between the two interfering SPPs will be the phase picked up upon reflection plus the one associated to their different path lengths along the metal:

$$\phi = 2k_p d + m\pi \quad (2)$$

According to Eq.(2), destructive or constructive interference should occur for those  $\phi$ -values equal to odd or even multiples of  $\pi$ , respectively. In these latter cases, the device would behave as an efficient source for unidirectional SPPs.

Note that Eq.(2) is based on two main simplifications. Firstly, the previous discussion is based on the reflection of SPPs by a groove array, while the electromagnetic (EM) fields radiated by the slit are, at short distances, more complex[15]. Secondly, Eq.(2) does not take into account the radiation from the grooves back into the slit while, in principle, EM-fields at all openings should be self-consistently calculated[17].

In order to check the validity of Eq.(2) we have carried out numerical calculations by means of both modal expansion [15] and Finite-Difference-Time-Domain (FDTD) [18] methods. FDTD is virtually exact for this type of 1D structures, as very small grid sizes can be used. On the other hand, the modal expansion treats only approximately the finite conductivity of the metal but provides a very compact representation for the EM fields, favouring the physical interpretation and, in some simple cases, the calculation of analytical expressions. We characterize the efficiency of the slit+groove system as SPP-launcher by the "enhancement factor",  $F_R$ , defined as the quotient between the current intensity of right propagating SPP ( $J_R$ ) with and without the grooves. Strictly speaking  $F_R$  provides the efficiency of the output side of the device; the total efficiency, defined as the percentage of laser beam energy transferred onto the plasmon channel, depends also on the lateral beam size, dielectric constant of the substrate, width of the metal film, corrugation on the input side, etcetera. Notice also that  $F_R > 2$  implies that, in the corrugated structure, the right propagating SPP carries more current than the total SPP current (left- plus right- moving) in the single slit case so, some or the power radiated out of plane is redirected onto the SPP channel.

The model system is a nano-slit SPP-launcher perforated on a gold film[19], designed to operate at a wavelength of 800 nm, inside the near infra-red range of EM spectrum. We

consider an array of 10 grooves with a period  $P = 390\text{nm}$ , obtained from Eq.(1) with  $m = 1$ . The depth of the grooves is chosen to be  $w = 100\text{nm}$ , while the width of both grooves and slit is  $a = 160\text{nm}$ , which are typical experimental parameters. Figure 2 renders the calculated (modal expansion: black curve, FDTD: blue curve) dependence of  $F_R$  with distance  $d$ . In this figure, vertical lines mark the locations of maximum interference predicted by Eq.(2). The agreement between the modal expansion and FDTD results is excellent, except for the behaviour at very short distances ( $d \approx 2a$ ), due to the cross coupling between the slit and the first groove through the vertical walls, which is neglected within the modal expansion. More importantly, the locations of maximum  $F_R$  are accurately predicted by Eq.(2), which allows us to design SPP-launchers without elaborate numerical calculations.

Notice that  $F_R$  would be 4 if the whole amplitude of the left-going SPP could be added constructively to the right-going one, while in our simulations a smaller value is always obtained. Calculations with the modal expansion show that this is due to the out-of-plane scattering of the left-going SPP by the array of grooves. The effect on  $F_R$  of both damping across the flat gold surface and partial transmission across the finite array plays a very minor role for the considered parameters.

In order to test experimentally our proposal, several samples were prepared with a Focused Ion Beam (FIB) in 300nm-thick gold films for different values for  $d$ , all other geometrical parameters being the same as in the previous calculations. Each sample consists of a single long slit flanked by a finite periodic groove array which extends over only half of the slit length (see Fig. 1a). This sample design allows the quantitative experimental study of the SPP launching efficiency, as the "isolated" slit (upper part) can be used as an in-chip reference. The set of samples was imaged by a Photon Scanning Tunneling Microscope (PSTM) making use of an incident focused beam illumination for frequencies in the [765, 800]nm interval. Due to specific features of the experimental set-up used for measurements in the optical regime, the incident laser beam was directed on the sample attached to a prism under an angle of  $43^\circ$  with respect to the normal. Notice, however, that the choice of angle of incidence is not critical for the spatial distribution of transmitted energy, as a sub-wavelength slit in an optically thick metal film transmits only the fundamental mode. For each distance  $d$ , a pair of images was recorded by scanning at a constant distance of about 60 to 80 nm from the sample surface. The first image of the pair, corresponding to the SPP launching by a single slit, is obtained by focusing the laser beam on the upper part of the

slit. For the second image, the laser beam is moved to the lower part in order to collect the data for the slit+grating case. Image pairs for  $d = 585\text{nm}$  and to  $d = 486\text{nm}$  are displayed in Figure 2b (left panels: single slit, right panels: slit+grating). Figure 2b clearly shows that the grating enhances the intensity of the right propagating SPP for  $d = 585\text{nm}$  whereas for  $d = 486\text{nm}$  this intensity is greatly reduced. In order to quantify this enhancement, an average longitudinal cross-cut of each image is obtained by using 20 longitudinal cross-cuts, corresponding to different coordinates along the slit axis. Then, the relative position of the two average cross-cuts composing each image pair is adjusted so that the saturated areas (i.e. the signal taken right on top of the slit) are super-imposed. Finally, the experimental enhancement factor,  $F_R$ , is extracted by averaging the ratio between the two curves along the longitudinal cross-cut. Figure 2a renders experimental results (squares) for  $F_R$  for the five different samples fabricated. Experimental data are in good agreement with the theoretical predictions, definitely showing that the presence of the grating modulates the coupling into the right propagating SPP. We find this agreement quite remarkable, especially when taking into account that each experimental point in Fig. 2a corresponds to a different sample.

We have also designed similar samples for efficient unidirectional SPP excitation at telecom (TC) wavelengths, increasing correspondingly the grating period and its separation from the slit. In this case, normal incidence back-side illumination is allowed by the experimental set-up and used in all experiments. The SPP propagation length is significantly longer in this wavelength range ( $\approx 200\mu\text{m}$ ) rendering a simple way of determining the enhancement factor. Similarly to the experiments described above, this factor has been obtained by using two near-field optical images taken at two positions of the focused laser beam incident normal to the sample surface (from the back side). The enhancement was simply determined as a power ratio between the SPP beams excited for two different adjustments, the SPP beam power being estimated far away ( $\approx 50\mu\text{m}$ ) from the slit. The typical near-field optical image obtained when illuminating the lower slit part (adjacent to the grating) is shown in Fig. 3 (upper panel), featuring a strong SPP beam propagating away from the slit in the direction opposite to that of grating and demonstrating thereby the desirable effect of the enhanced unidirectional SPP excitation.

It should be mentioned that the enhancement factor determined in this way exhibited a significant dispersion due to inaccuracy in the illuminating laser beam adjustment. Consequently, several series of measurements were performed conducting independent adjustments

for each sample and wavelength. Averaged results and estimated errors are shown in Fig. 3, which shows the wavelength dependence of the SPP excitation enhancement caused by the grating array. As can be seen, the comparison between theory and experiments is rather satisfactory: for the case of the sample with  $d = P + P/2 = 1125$  nm, the enhancement factor decreases as the wavelength increases (with the only exception of a sharp peak at 1520 nm), evolving from an enhanced regime ( $F_R \approx 2$ ) to one in which SPP coupling is clearly diminished by the grating ( $F_R < 1$ ). On the other hand,  $F_R \approx 2$  all over the range for the sample with  $d = P - P/4 = 562$  nm, as predicted by the modal expansion calculation.

Another application of the system proposed in this paper is the focusing of SPPs, creating local field enhancement ("hot spot") at a given location. Focusing of SPP has been achieved through the interaction of SPP with curved surface corrugations[20, 21, 22, 23, 24]. The proposed approach for the localized unidirectional excitation of a SPP beam can be generalized to focus SPPs with a higher efficiency than in the cited study while, at the same time, blocking the propagation away from the focus. Importantly, in these curved structures, the rigorous modelling of the SPP excitation needed for optimization of the focusing would be difficult, while the relation given by Eq.(2) still provides simple design rules. As a proof of principle, in this paper we present focusing at telecom wavelengths by milling a curved slit along with the corresponding grating grooves [Fig. 4(a)], using a similar configuration to that illustrated with the near-field optical image shown in Fig. 3. The effect of SPP beam focusing was clearly seen already at the stage of far-field adjustment (using a microscope arrangement with an infrared CCD camera) due to weak out-of-plane SPP scattering by surface roughness [Fig. 4(b)]. The typical near-field optical image obtained at the wavelength of 1520 nm demonstrates efficient focusing of a launched SPP beam at the center of slit curvature with a spot size of  $2.5 \times 2.5 \mu\text{m}^2$  [Fig. 4(c)]. More generally, the design of other more complicated curved structures based on these principles can be envisaged allowing, for example, the excitation of SPP beams propagating in different directions and focused at different locations. Further investigations in this direction are being conducted.

In conclusion, we have studied the SPP launching by subwavelength slit apertures with back-side illumination, demonstrating a novel method allowing for efficient localized unidirectional generation by means of a finite grating of grooves adjacent to the slit. Our simple model enables us to make quantitative predictions that have been experimentally confirmed for both near infrared and telecom ranges. Such analytical predictions on coupling-

enhancement have also been found in good agreement with sophisticated computer simulations, irrespective of our model's simplified description of some of the physics involved. With respect to practical applications, we have shown that the SPP coupling-in can be enhanced by a factor of 3 without any modification on the illumination source. This is particularly relevant if we keep in mind that the total transmitted current can also be easily enhanced making use of a symmetric grating at the illuminated surface [25]. Moreover, the SPP beam is confined only at one side of the aperture and it can also be suppressed with a careful selection of the geometrical parameters. We have also shown how a slight modification of the system can be used to concentrate freely propagating SPP's in region with lateral dimensions comparable to the SPP wavelength. In our opinion, the possibility of efficient local SPP excitation producing a well defined and collimated SPP beam is of great importance and extremely useful for various plasmonic devices of current interest.

- 
- [1] Barnes W. L., Dereux A. & Ebbesen T. W. Surface plasmon subwavelength optics. *Nature* **424**, 824 (2003).
  - [2] Ozbay E. Plasmonics: Merging photonics and electronics at nanoscale dimensions. *Science* **311**, 189 (2006).
  - [3] Otto, A. Excitation of nonradiative surface plasma waves in silver by the method of frustrated total reflection. *Z. Phys.* **216**, 398 (1968).
  - [4] Lamprecht B., Krenn J. R., Schider G., Ditlbacher H., Salerno M., Felidj N., Leitner A., Aussenegg F. R. & Weeber J. C. Surface plasmon propagation in microscale metal stripes. *Appl. Phys. Lett.* **79**, 51 (2001).
  - [5] Ritchie, R. H., Arakawa, E. T., Cowan J. J. & Hamm R. N. Surface-plasmon resonance effect in grating diffraction. *Phys. Rev. Lett.* **21**, 1530 (1968).
  - [6] Ditlbacher, H., Krenn J. R., Felidj N., Lamprecht B., Schider G., Salerno M., Leitner A. & Aussenegg F. R. Fluorescence imaging of surface plasmon fields. *Appl. Phys. Lett.* **80**, 404 (2002).
  - [7] Sönnichsen C., Duch A. C., Steininger G., Koch M., von Plessen G. & Feldmann J. Launching surface plasmons into nanoholes in metal films *Appl. Phys. Lett.* **76**, 140 (2000).
  - [8] Devaux E., Ebbesen T. W., Weeber J.C. & Dereux A. Launching and decoupling surface

- plasmons via micro-gratings. *Appl. Phys. Lett.* **83**, 4936 (2003).
- [9] Yin L., Vlasko-Vlasov V. K., Rydh A., Pearson J., Welp U., Chang S. -H., Gray S. K., Schatz G. C., Brown D. E. & Kimball, C. W. Surface plasmons at single nanoholes in Au films. *Appl. Phys. Lett.* **85**, 467 (2004).
- [10] Popov E., Bonod N., Neviere M., Rigneault H., Lenne P. F. & Chaumet P. Surface plasmon excitation on a single subwavelength hole in a metallic sheet. *Appl. Opt.* **44**, 2332 (2005).
- [11] Agrawal A., Cao H. & Nahata A. Excitation and scattering of surface plasmon-polaritons on structured metal films and their application to pulse shaping and enhanced transmission. *New J. Phys.* **7**, 249 (2005).
- [12] Chang S. H., Gray S. K. & Schatz G. C. Surface plasmon generation and light transmission by isolated nanoholes and arrays of nanoholes in thin metal films. *Opt. Express* **13**, 3150 (2005).
- [13] Lalanne P., Hugonin J. P. & Rodier C. Theory of surface plasmon generation at nanoslit apertures. *Phys. Rev. Lett.* **95**, 263902 (2005).
- [14] Bozhevolnyi S. I., Boltasseva A., Sondergaard T., Nikolajsen T. & Leosson K. Photonic bandgap structures for long-range surface plasmon polaritons. *Opt. Commun.* **250**, 328 (2005).
- [15] Lopez-Tejiera F., Garcia-Vidal F. J. & Martin-Moreno L. Scattering of surface plasmons by one-dimensional periodic nanoindented surfaces. *Phys. Rev. B* **72**, 161405(R) (2005).
- [16] Gonzalez M. U., Weeber J.-C., Baudrion A. L., Dereux A., Stepanov A. L., Krenn J. R., Devaux E. & Ebbesen T. W. Design, near-field characterization, and modeling of  $45^\circ$  surface-plasmon Bragg mirrors. *Phys. Rev. B* **73**, 155416 (2006).
- [17] Martin-Moreno L., Garcia-Vidal F. J., Lezec H. J., Degiron A. & Ebbesen T. W. Theory of highly directional emission from a single subwavelength aperture surrounded by surface corrugations. *Phys. Rev. Lett.* **90**, 167401 (2003).
- [18] Taflove A. & Hagness S.C. *Computational Electrodynamics: The Finite-Difference Time-Domain Method* (Artech House, Boston, 2000).
- [19] The dielectric constant for gold was taken from Vial A., Grimault A., Macias D., Barchesi D. & de la Chapelle M. Improved analytical fit of gold dispersion: Application to the modeling of extinction spectra with a finite-difference time-domain method. *Phys. Rev. B* **71**, 085416 (2005).
- [20] Nomura W., Ohtsu M. & Yatsui T. Nanodot coupler with a surface plasmon polariton condenser for optical far/near-field conversion. *Appl. Phys. Lett.* **86**, 181108 (2005).



- [21] Yin L., Vlasko-Vlasov V. K., Pearson J., Hiller J. M., Hua J., Welp U., Brown D. E. & Kimball C. W. Subwavelength focusing and guiding of surface plasmons. *Nano Letters* **5**, 1399-1402 (2005).
- [22] Liu Z., Steele J. M., Srituravanich W.; Pikus Y.; Sun C. & Zhang X. Focusing surface plasmons with a plasmonic lens. *Nano Letters* **5**, 1726-1729 (2005).
- [23] Offerhaus H. L., van den Bergen B., Escalante M., Segerink F. B., Korterik J. P. & van Hulst N. F. Creating focused plasmons by noncollinear phasematching on functional gratings *Nano Letters* **5**, 2144-2148 (2005).
- [24] Steele J. M., Liu Z., Wang Y. & Zhang X. Resonant and non-resonant generation and focusing of surface plasmons with circular gratings. *Opt. Express* **14**, 5664 (2006).
- [25] Garcia-Vidal F. J., Lezec H. J., Ebbesen T. W. & Martin-Moreno L. Multiple paths to enhance optical transmission through a single subwavelength slit. *Phys. Rev. Lett.* **90**, 213901 (2003).

## I. ACKNOWLEDGEMENTS

Financial support by the EC under Project FP6-2002-IST-1-507879 (Plasmo-Nano-Devices) is gratefully acknowledged. We thank J. Dintinger and J.-Y. Laluet for technical assistance.

## II. COMPETING FINANCIAL INTERESTS

The authors declare that they have no competing financial interest.

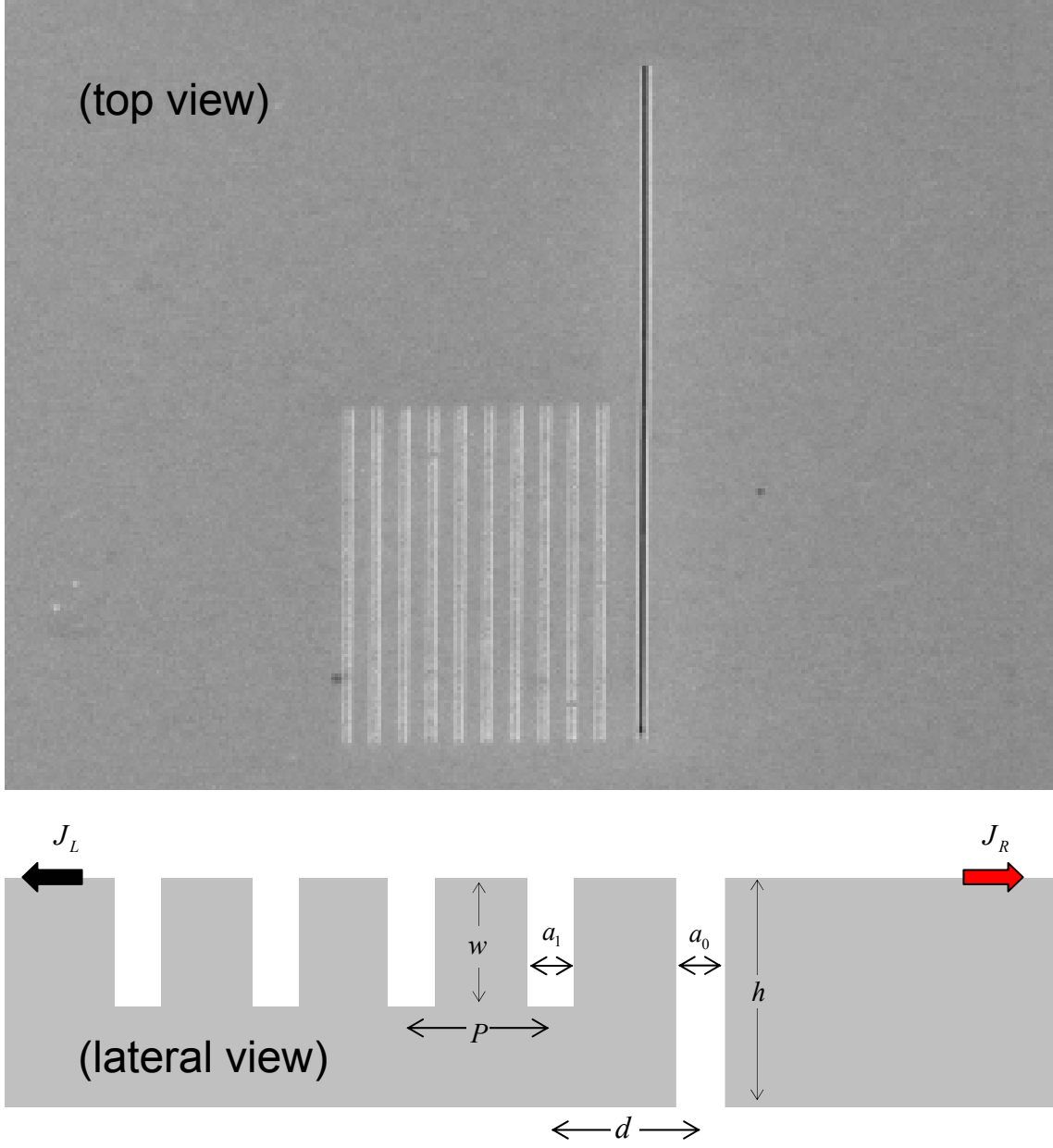


FIG. 1: SEM and schematic pictures of the structures investigated. Parameters used in the definition of the slit, grooves and metal film are also shown.  $J_R$  and  $J_L$  stand for the current energy densities for right- and left- propagating surface plasmons, respectively

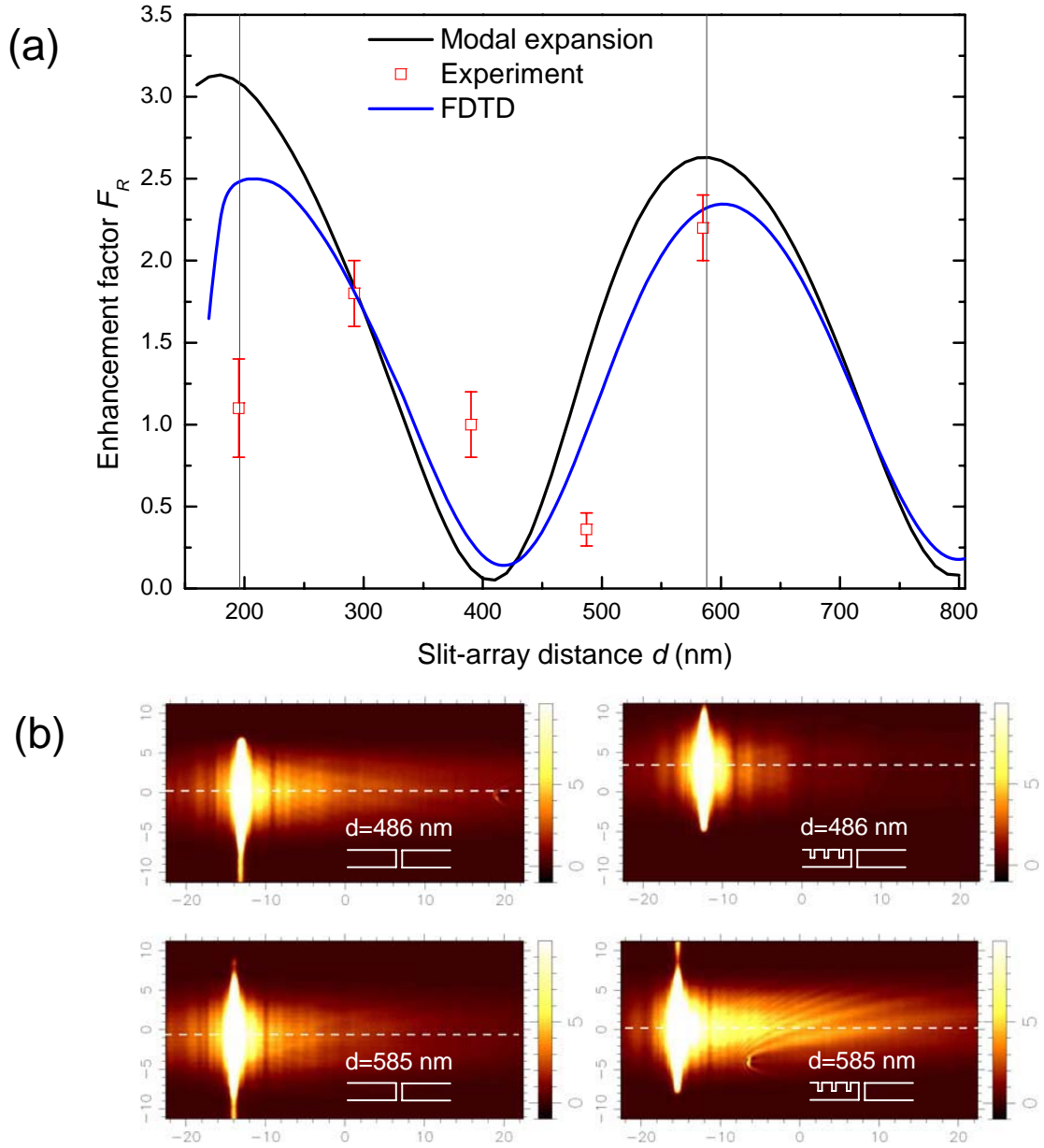


FIG. 2: (a) Dependence with slit-array distance of the enhancement factor  $F_R$ . The working wavelength is  $\lambda = 800$ nm, while the geometrical parameters defining the system are: slit length is  $30\mu m$ , slit and groove widths  $a = 160$ nm, groove depth  $w = 100$ nm and array period  $P = 390$ nm. The figure renders the computed results obtained by both modal expansion (black line) and FDTD methods (blue line). Vertical lines mark the positions of the enhancement maxima according to Eq. (2). Experimental results are represented by squares. (b) PSTM images recorded at  $\lambda = 800$ nm for two different slit-grating distances. Left column: isolated slit. Right column: slit+grating.

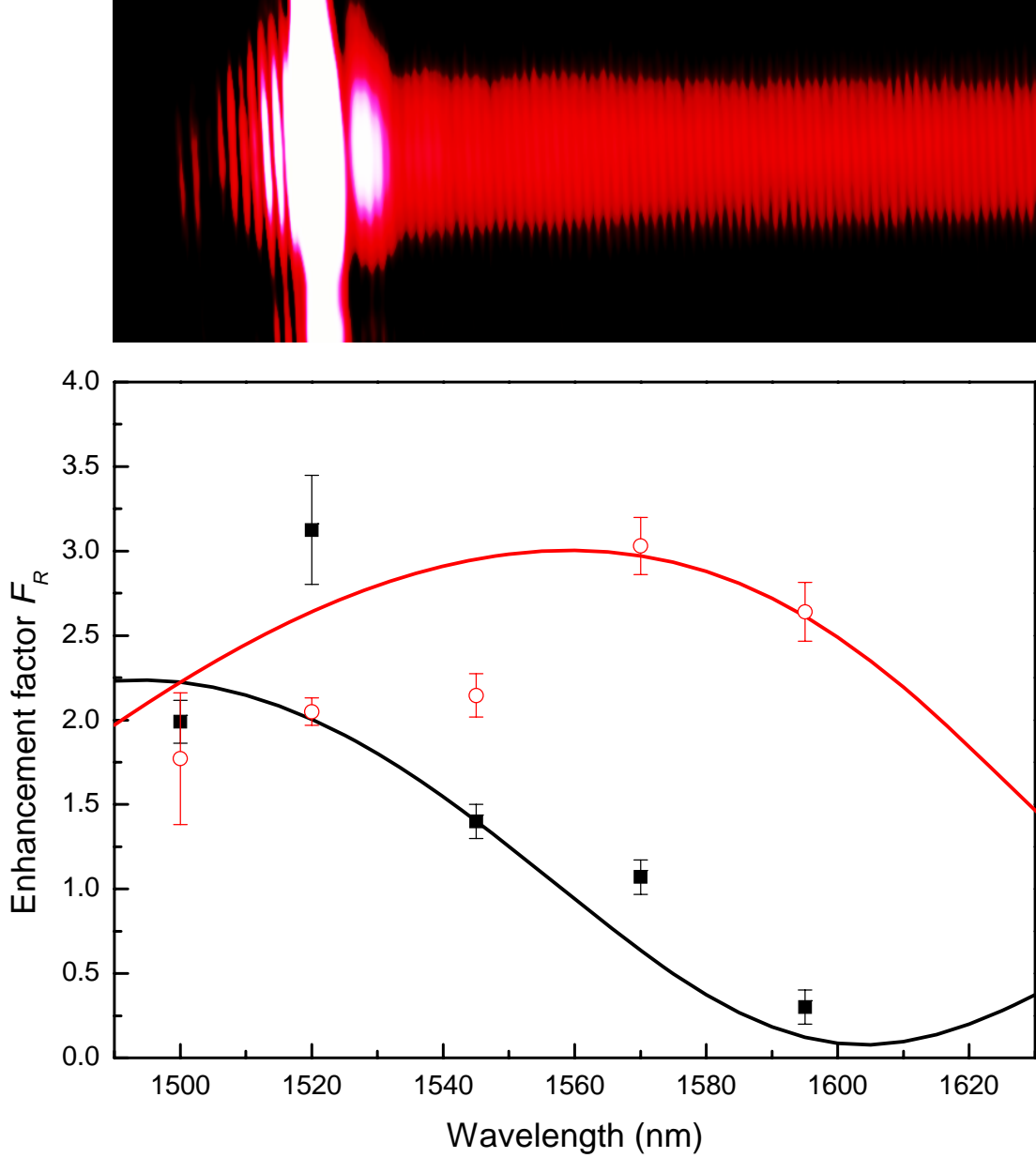


FIG. 3: Experimental results and modal expansion calculations for the spectral dependence of the enhancement factor at the telecom range. Two samples were considered. In both, the slit length is  $50\mu\text{m}$ , slit and grooves widths are 400 and 200nm, respectively, with groove periodicity  $P = 750\text{nm}$ , film thickness  $h = 300\text{nm}$  and groove depth  $w = 100\text{nm}$ . In one sample the slit-grating distance  $d = 3P/2 = 1125\text{nm}$  (experiment: black squares, theory: black curve) while, in the other  $d = 3P/4 = 562\text{nm}$  (experiment: red circles, theory: red curve) The image in the upper panel depicts grating induced enhancement for  $d = 3P/2$  at  $\lambda = 1520\text{nm}$ . (Size =  $70 \times 26\mu\text{m}^2$ ). Weak periodic modulation of the strong SPP beam propagating to the right (upper panel) is due to its interference with a SPP wave reflected by a remote auxiliary structure.

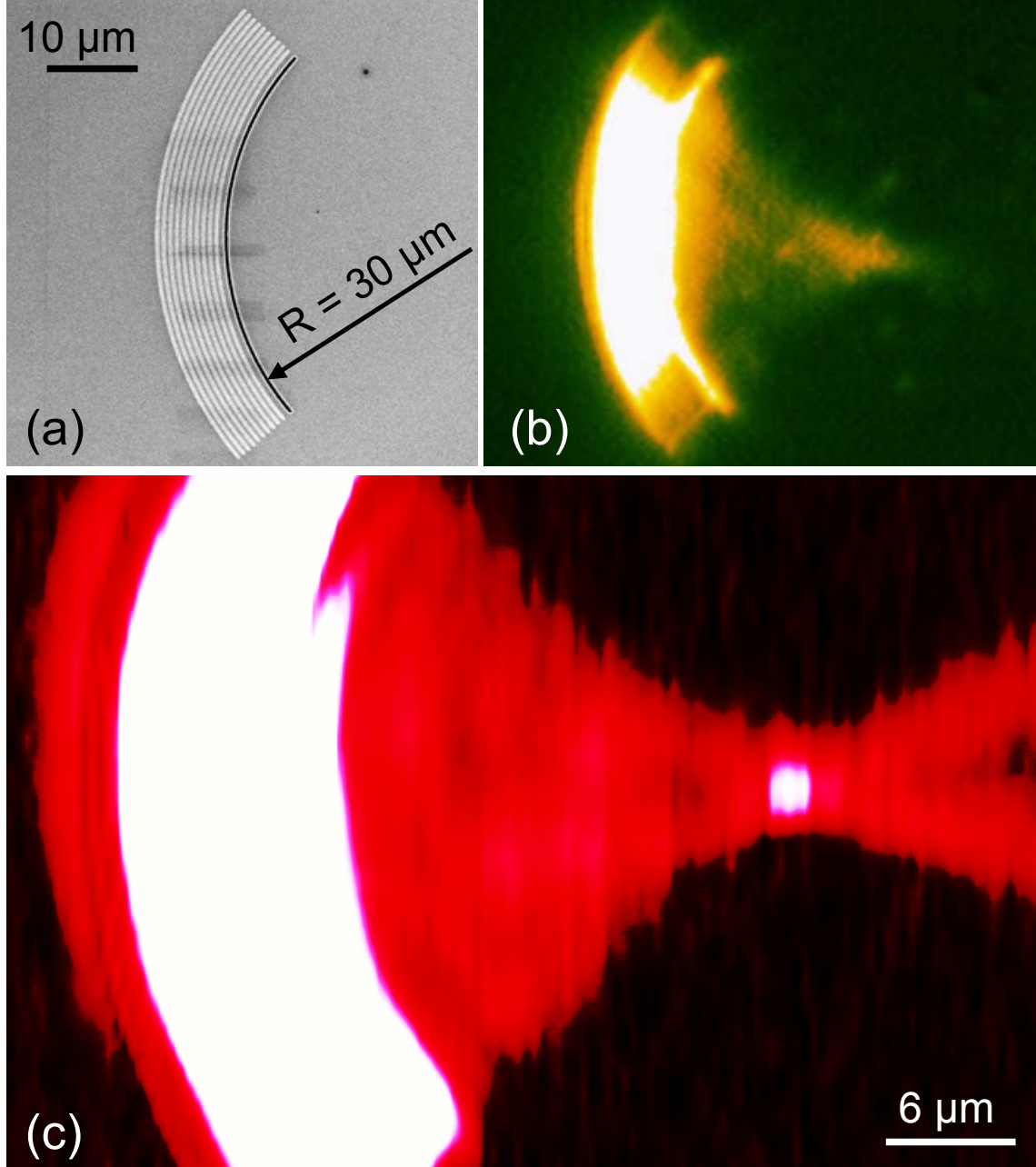


FIG. 4: Demonstration of the simultaneous SPP excitation and focusing using a curved slit flanked with concentric periodic grooves. (a) SEM image of the fabricated structure characterized by the slit and groove widths of 400 and 200 nm, respectively, groove periodicity of 750 nm, groove depth of 100 nm and slit-groove distance of 1125 nm. Film thickness is 280 nm and curvature radius is 30  $\mu$  m. The slit chord length is 40  $\mu$  m. (b) Far-field image recorded with a CCD-camera and (c) the corresponding near-field optical image (size =  $48 \times 32 \mu\text{m}^2$ ), both being obtained when the curved slit was illuminated at normal incidence with radiation at the telecom wavelength of 1520 nm.